Isothermal Calorimetry: Molecular Interactions between Small Molecules in Organic Solvents

Raquel Gutiérrez-Climente, Elise Prost, Aude Cordin, Carlos Chesta, Luminita Duma

Book Chapter Template

Isothermal calorimetry: molecular interactions between small molecules in organic solvents

Raquel Gutiérrez-Climente‡,[1] Elise Prost‡,[2] Aude Cordin,[2] Carlos Chesta,[3] Luminita Duma*,[4]

[1] IBMM, Univ. Montpellier, CNRS, ENSCM, Montpellier, France.

[2] University of Technology of Compiègne, UPJV, UMR CNRS 7025, Enzyme and Cell Engineering, Research Centre Royallieu, Compiègne, France.

[3] National Universiy of Río Cuarto, IITEMA-CONICET, 5800 Río Cuarto, Argentina.

[4] Champagne-Ardenne University, CNRS, ICMR UMR 7312, 51097 Reims, France.

‡ These authors equally contributed to this work.

* Correspondence: luminita.duma@univ-reims.fr

Abstract

Isothermal titration calorimetry (ITC) is widely used to study protein-ligand, DNA-drug and/or protein-protein interactions but its application for small molecule complexation remains limited namely when the titration is performed in organic solvents. Compared to other dedicated spectroscopic techniques like nuclear magnetic resonance, infrared spectrometry or fluorimetry, which require a series of experiments to extract site-specific stoichiometry and affinity information, ITC provides in a single experiment a complete thermodynamic picture of the overall interaction mechanism. This chapter presents examples that support the high potential of ITC to probe interactions between small molecules in methanol, acetonitrile and methanol/water mixture on a Nano ITC Low Volume device (TA Instruments), with an emphasis on both simple (1:1) and more complex (1:1 and 1:2) interaction mechanisms.

Keywords: Isothermal calorimetry, thermodynamics, association constant, stoichiometry, small molecules, non-aqueous solvents

1. Introduction

Molecular recognition processes, omnipresent in nature, are of crucial importance in all living species. The magnitude of any molecular interaction, which can be translated in terms of heat released or adsorbed, can vary depending on the chemical nature of the interacting partners, on their concentration and the solvation environment in which the process takes place. Developed originally in the middle of the 1960s [1] for studying chemical reactions [2], ITC can measure with high precision and accuracy the heat energy associated with intermolecular reactions but also solvation and dilution experiments. Over the years, ITC became gradually widespread and popular to characterize the thermodynamics signature of molecular interactions in drug design [3,4], in which the knowledge of the thermodynamic parameters in combination with the structural and kinetic information is decisive during the hit-to-lead optimization, an early step in the drug design

process. At this optimization stage, hundreds of compounds with promising affinity against the protein target are screened to identify the best one or two candidate molecules, usually from different chemical series [5]. Compared to other methods employed in the field of drug discovery, ITC offers two clear advantages facilitating the selection of the candidate molecules: On one side, ITC is the only method that directly measures the reaction enthalpy change [6], which can be considered as an interaction descriptor [7] and therefore an extremely useful parameter for structure thermodynamics correlations. It offers a valuable information notably for the compounds having similar binding affinities but different thermodynamic parameters [7,8]. Traditionally, drugs characterized by an enthalpy-driven binding were preferred [7,9]. Nevertheless, the nature of the binding site deserves to be considered because, when an apolar part of the drug interacts with an apolar region of the protein target, the entropic contribution will be favored and the reaction becomes entropy-driven [10]. On the other side, thanks to the detection of the heat change in water molecules and the transfer of protons of the drug molecule during the solvation and dilution experiments, ITC illustrates the differences between polar and apolar interactions that are invisible using techniques such as X-ray crystallography and surface plasmon resonance (SPR) [10]. All these advantages are also highly valuable for other ITC applications such as enzyme-catalyzed reactions [11] and host-guest supramolecular complexation [12]. In supramolecular chemistry for example, ITC combined with supramolecular structure information can provide deeper information on the energies associated with non-covalent interactions (hydrogen bonding, electrostatic, π-π stacking, cation-π and anion-π interactions) and the hydrophobic effect induced by the displacement of water molecules [13].

Recently, the technique appeared also particularly useful and versatile in kinetic assays [14] where the direct measurement of a catalytic reaction [15,16] was possible. Other applications include the monitoring of microbial activity and dynamics [17,18], the stability assessment of (bio)pharmaceuticals [19], etc. The development of Low Volume (LV) Nano ITC calorimeters should extend the application fields of this technique not only to biomolecules available in small amounts but also to the study of complexation reactions in organic solvents thanks for example to the availability, on the same calorimeter, of a standard buret handle for aqueous solutions and organic solvents compatible buret handle.

The main advantage of ITC, when compared to other interaction-study dedicated spectroscopies, like nuclear magnetic resonance (NMR), Fourier transform infrared (FTIR) spectrometry or fluorimetry, is the ability to provide in a single experiment the entire thermodynamic profile of the investigated interaction process. In practice, an ITC experiment measures accurately the heat released or adsorbed when a molecule solution is titrated into another in a given aqueous or non-aqueous solution. The large majority of ITC measurements is conducted in aqueous solutions to study protein-ligand, DNA-drug and/or protein-protein interactions [10] whereas most of the ITC investigations in organic solvents or non-aqueous/aqueous mixtures focus on the solvation or dissolution thermodynamic study of various small molecules [20–23], drugs [24], single amino acids [25–27], small peptides [28], metal ions [29], etc. It worth noting also some complexation studies for copper ions with β-alanine in ethanol [30], 15-crown-5 ether with Na^+ in water-ethanol [31], 18-crown-6 with triglycine in water-acetone and water-dimethyl sulfoxide [32], β-cyclodextrin with benzoic acid in water-ethanol [32], fluorescein isothiocyanate with polymers in water-methanol [33], and the association analysis of urea-based supramolecular polymers in different solvents [34].

The scarce resources in past calorimetry or contemporary ITC literature about intermolecular interactions in organic solvents prompted us to write this chapter. After a brief introduction of the main basic concepts, we will show the ITC characterization of several 1:1 and 1:2 complexes in organic solvents together with the analysis of the data and the results which provide the thermodynamic profile, stoichiometry and association constant of the reaction. The correlation of ITC results with association or structural

information from other spectroscopies may help understanding the formation of even more complex binding events.

2. Isothermal calorimetry: general principles and experimental details

Calorimetry measures the changes in heat released or absorbed during a chemical reaction or a physical process. Heats are measured with instruments called calorimeters classified as adiabatic or isothermal [35]. Heat measured on adiabatic devices show a permanent increase or decrease in temperature. The temperature changes thus obtained are directly related with the heat capacity of the instrument which therefore requires the acquisition of distinct experiments for calibration. In isothermal calorimeters the heat is allowed to flow between the reaction cell and a heat sink surrounding the two cells (see Figure 1a) and is actively regulated to maintain a constant level by power compensation. The development of micro- and nano-calorimetry rendered possible the detection of very small heat changes in small volumes of samples. Nano calorimeters have a detection limit in the nanowatt range [35]. Historically, it has been applied to the study of the reactants available in reduced amounts like biomolecules.

The design of the NanoITC from TA Instruments relies on the differential power compensation technology (see Figure 1a) which allows to optimize sensitivity and responsiveness. Nanowatt sensitivity is achieved thanks to an internal reference. Two cylinder-shaped identical chambers (also called sample and reference cells) of 170 µL are located in a compartment which works as a thermal barrier. As described in the user manual [36], semiconducting thermoelectric devices (or TED) control and detect temperature differences between the sample and the reference chambers. In a titration experiment, both cells are entirely filled: the reference cell with the pure solvent, the sample cell with one reactant (or titrand) and the syringe with the other reactant (or titrant) of the reaction under study, both in the same solvent. The titrant is usually prepared at 10-fold higher concentration for a 1:1 binding model [37]. ITC titration experiments are implemented by incremental injection of a precise volume of titrant into the solution of titrand at discrete time intervals (see Figure 1c). Typically, about 25 injections per experiment are performed using a motor-driven syringe capable to deliver defined volume within 1-10 µL per injection. The syringe is coaxially introduced in the sample cell through a long access tube. The stepping motor precisely controls not only the injection volume but also the stirring speed of the reactants in the sample cell. Therefore, for each injection, the interaction between the two reactants releases (or adsorbs) heat that increases (or decreases) the sample cell temperature. This temperature change will activate the feedback heat controller (power compensation) on the sample cell such as to maintain a zero temperature difference between the two cells. For each heat variation during a stepwise titration, the feedback regulator will compensate this difference by decreasing (or increasing) the heat of the sample cell by the amount of heat supplied by the reaction and, at each variation associated to each injection step, will lead to a peak in the thermogram. Figure 1c illustrates the construction of a representative thermogram as the stepwise titration proceeds. During the titration experiment, the reactant in the sample cell is gradually transformed into the molecular complex. The injection of the titrant is conducted until the titrand in the sample cell is fully saturated and the heat signal becomes equal to the background heat generally equal to the dilution heat of the titrant [37].

The normalized integrated area of each peak is next approached with the appropriate model to estimate the affinity, enthalpy and stoichiometry of the interaction. The first recorded experiment can be further analyzed with the Experiment Design tool of NanoAnalyze to find out the optimal concentration conditions leading to a “S-shape” thermogram (see Figure 1b). The titration experiment is then repeated with these optimized concentrations and the data analyzed. The integration of each peak area in the thermogram (Figure 1b top) gives the amount of heat exchanged while injecting a known amount of the reaction partner into the sample cell. When the concentrations in the syringe and the sample

cell were appropriately chosen, a display of the integrated heat signal as a function of mole ratio (of the injected compound over the one contained in the sample cell) reveals a typical sigmoidal shape (Figure 1b bottom). An inspection of the integrated titration curve gives information on the molar enthalpy (ΔH) from the height of the curve, the number of binding sites (or stoichiometry) of the reaction from the position of the inflection point on the mole ratio axis, and the association constant (K_a) from the slope of the curve. Nowadays, the companies provide an analysis software that incorporates the specifics of the instrument. It is therefore relatively easy to make a first estimation of the ΔH, n and K_a quantities thanks to various models that approach the experimental data using a nonlinear routine to find the most probable thermodynamic parameters describing the interaction process.

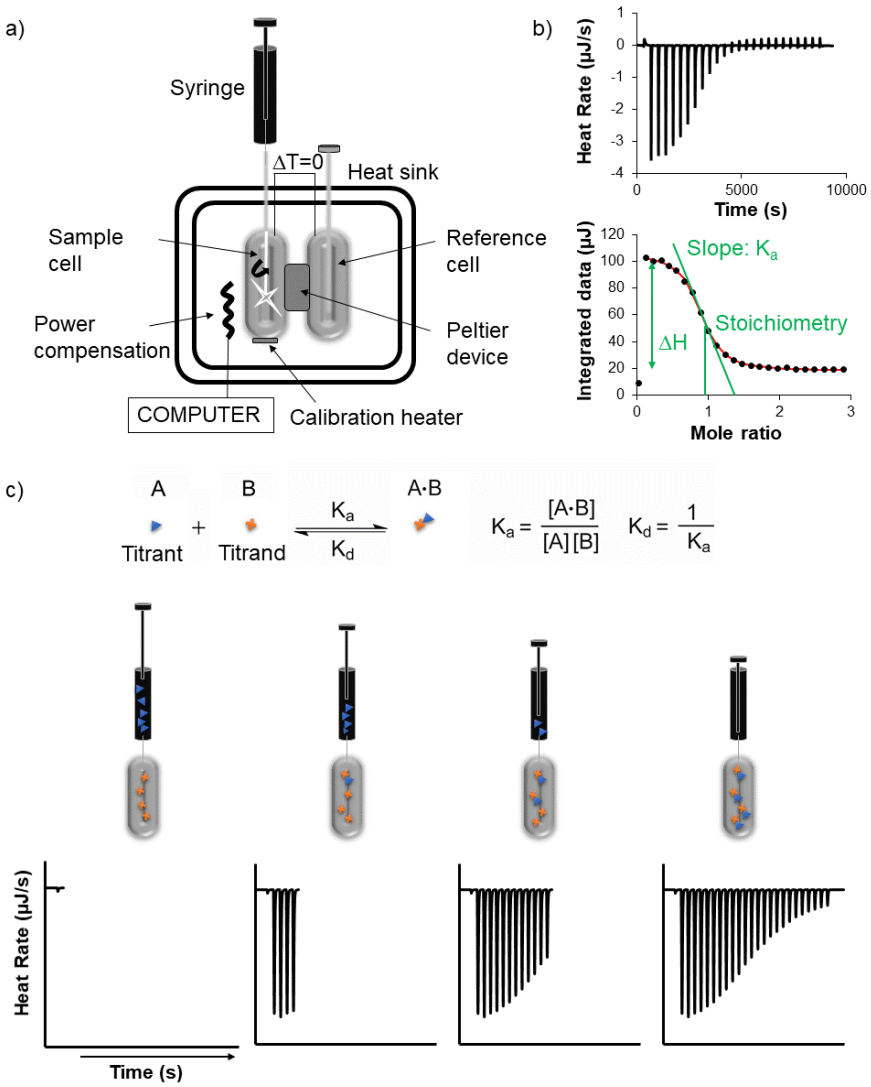

Figure 1: a) Drawing of the Nano ITC measuring unit (TA Instruments) and its basic elements. b) Typical stepwise ITC raw thermogram and the corresponding integrated data. The parameters obtained after adjusting the data with the one-site binding model are also highlighted in green. c) Chemical reaction and illustration of the evolution of the stepwise raw thermograph as the titrant is injected in the sample cell.

In the absence of any solubility or aggregation issues, direct and reverse titration [38,39] can be considered when studying the interaction of small molecules in a given solvent. For two A and B interacting molecules (Figure 1c), the injection of aliquots of A

into B is called direct titration whereas the injection of aliquots of B into A is termed reverse titration. As previously mentioned, the titration experiment is well performed when the concentrations are chosen such as the molecule in the sample cell is fully saturated. Assuming that the molecular mass of reactants does not affect the equilibrium binding equations (microscopy reversibility), direct and reverse titrations should be equivalent. They can be modeled by the same set of equations and should lead to the same thermodynamic parameters for a reversible reaction.

The reaction in Figure 1c corresponds to a complex where a single molecule A interacts with a single molecule B (i.e., the one to one model which corresponds to a stoichiometry of 1). Since the reaction enthalpy change (ΔH) and association constant (K_a) are directly measured from an ITC titration experiment, under constant temperature and pressure, the Gibbs free energy (ΔG) and the entropy (ΔS) can obtained using the following relationships:

$$\begin{cases} \triangle G = \triangle H - T \triangle S \\ \triangle G = -RTlnK_a \end{cases} \quad \text{(Eq 1)}$$

with R the ideal gas constant (R = 8.314 J/mol·K) and T the temperature in K. Equilibrium association constants can be obtained with acceptable statistical precision if the following condition is fulfilled:

$$1 < c < 1000 \quad \text{(Eq 2)}$$

where *c* (also known as *c*-value) is given by the relationship $c = nK_a[B]$, [B]: concentration of B molecule [40]. The condition in Eq. 2 is directly related to the shape of the binding curve (also termed thermogram). For protein-ligand complexes generally characterized by an affinity in the µM range (i.e. 10^6 M^{-1} Ka), a *c*-value within 20 and 200 is recommended in order to minimize K_a errors and thermodynamic parameters as shown by comparing ITC reports from different laboratories on the same benchmark protein-ligand complex in buffer [41–43].

By performing the ITC titration experiment at different temperatures, the change in heat capacity, ΔC_p, for the A·B complex formation can be estimated according to the following equation:

$$\Delta C_p = \frac{d\Delta H}{dT} \quad \text{(Eq 3)}$$

with ΔC_p in J/mol·K.

The enthalpy represents the energy change of the system when the molecule A interacts with B in a given solvent. Different type of noncovalent interactions (hydrogen bonds, ions pairs, van der Waals forces, etc.) can take place at the binding interface and therefore affect the enthalpy change. For example, the formation of noncovalent interactions between atoms is an exothermic process characterized by a negative enthalpy change whereas their breaking is an endothermic one with a positive enthalpy change. The heat released during a binding process describes the entire system under study with individual contributions from the interacting partners but also the solvent. In reality, the measured enthalpy change upon binding is the sum of many positive and negative ΔH contributions resulting from the simultaneous formation and disruption of noncovalent interactions [44]. Like in protein-ligand interactions in an aqueous medium, the observed ΔH of binding in an organic solvent is a global property which reflects the partial loss of solvent contacts of the interacting partners, the formation of complex noncovalent interactions and the solvent rearrangement near the complex surface.

As main direct experimental observable in calorimetry, the measured heat is correlated with the reaction taking place at the molecular level and the aim of the calorimetry is to provide reliable heat data capable to characterize molecular interactions. In the literature, the enthalpies directly obtained by calorimetry have been correlated with the values of binding enthalpy derived from the van't Hoff relationships. Experimental and simulation studies have shown that statistically relevant discrepancies are notably found when the experimental setup or data analysis are not correctly performed [45,46].

Incremental titration described previously is the most common titration method used. Continuous titrations, which consists of constantly injecting the titrant into the calorimeter vessel while monitoring the thermal power, are shorter than the incremental ones and therefore, they can be of great interest for unstable samples. The development of the continuous ITC (cITC) method for micro- and nano-calorimeters [47] rendered the technique even faster and more versatile for the study of thermodynamic processes in a complex interaction. Interestingly, it can also represent a quick alterative to find out the concentration conditions leading to an exploitable thermogram. The screening of the optimum conditions (Eq 2) may be speeded up even more if the cITC thermograms can be exploited by the Experiment Design tool in NanoAnalyze software, as mentioned for the classical ITC data. Unfortunately, this is not yet the case with the currently available NanoAnalyze software (3.12.0).

Another advantage of the cITC, is the potential expansion of the equilibrium constants accessible by ITC. Indeed, Markova and Hallén [47] have shown by computer simulations that cITC expands by 3 orders of magnitude the range of K_a achievable by ITC. Therefore, for cITC the Eq 2 becomes:

$$1 < c < 3x10^{6} \qquad \text{(Eq 4)}$$

with 10^{12} M^{-1} being the highest equilibrium constant reachable by cITC. This is rendered possible by the increased data points density in a continuous titration experiment which better defines the slope region in a 1:1 binding curve.

3. Experimental details

The reagents used in this work are summarized in Table 1. All measurements were performed on a differential power compensation Nano ITC Low Volume (Nano ITC LV) calorimeter from TA Instruments (Waters, France), using a 50 µL injection syringe while stirring at 400 rpm (the maximum stirring value). The Nano ITC LV has two gold 170 µL reaction vessels and a buret assembly holding a stainless-needle syringe with a twisted paddle at the tip and titrant exit at the bottom. Therefore, the syringe serves not only for the delivery of the titrant but also for stirring. To avoid the formation of bubbles in the cells and syringe, the samples were degassed in a vacuum degassing station [48] for 15 minutes immediately before use. Injections were started after achievement of baseline stability (using the automatic equilibration mode for "small Heats" of ITCrun program controlling the calorimeter with the following criteria: absolute acceptable slope: ΔH 0.1µW/h; acceptable absolute standard deviation: 0.01 µW). In addition, an equilibration time of 300 s has been considered before the first and after the last injection to assess the quality of the baseline. The experimental parameters were: 350 µL in the sample cell, 50 µL in the syringe, 350 µL solvent in the reference cell (changed weekly), 25 injections of 2.02 µL except for the first injection which was of 0.48 µL. The integrated heat effects of each injection were corrected by subtraction of the corresponding integrated heat effects associated with titrant dilution into the solvent. The experimental data obtained from the corrected calorimetric titration were analyzed on the basis of different interaction models with the NanoAnalyze software. The first injection was not taken into consideration for data analysis.

Table 1: Reagents used in this work.

Name	Purity %	Supplier	Reference	CAS number
Acetonitrile	99.95	Biosolve	UN1648	75-05-8
Benzoic acid	≥ 99.5	Sigma-Aldrich	242381-25G	65-85-0
DMAPMAm [a]	99	Aldrich	409472-250ML	5205-93-6
Glucuronic acid	≥ 98	Sigma	G5269	6556-12-3
Isophthalic acid	99	Alfa Aeser	A14445	121-91-5
Methanol	100	VWR	20847-320	67-56-1

[a] *N*-[3-(dimethylamino)propyl]methacrylamide

The electrical calibration of the calorimeter was performed according to the manufacturer's instructions. Water in water dilution experiments are regularly performed to check and validate the initial criteria of the manufacturer. Cells and syringe correct cleaning is essential to avoid artifacts and produce good quality data. Additionally, it is crucial to keep the needle of the syringe perfectly straight. Cleaning of the sample cell can be performed automatically using the vacuum of the degassing device and is generally done with 1 L of 2.5 % DECON followed by 1 L of MilliQ water. An ITC experiment takes between 1 and 2 hours depending on the injection delay and the equilibration duration necessary to fulfill the heat stability statistical criteria. ITCRun, the software which controls the Nano ITC calorimeter, doesn't record the evolution of the heat values during the equilibration delay but only its duration.

Despite the relative simplicity of ITC experiments, the selection of the right binding model for the fitting of the experimental data in order to estimate the thermodynamic parameters can be challenging, especially for complexes where one of the reactants present multiple sites and there is not previous information about the stoichiometry or binding mechanism [49]. Among the various softwares currently available for the titration data analysis, the softwares provided by the ITC manufacturers, i.e. Origin from MicroCal/Malvern and NanoAnalyze in the case of TA instruments, the interpretation of the binding isotherms can be done for each data set individually using either classical models such as one-site independent or two-sites sequential models, multiple sites, dimer dissociation, cooperative and competitive replacement models. The possibility of dilution subtraction or the selection of a control model together with the binding model remains at the user's choice.

Over the last decade, alternative softwares have been developed for more complex processes, e.g. AFFINImeter [50], pytc [51], HypΔH [52], CHASM [53] or SEDPHAT [54]. The free platform SEDPHAT gives the possibility to combine several experimental data (calorimetry, spectrophotometry, sedimentation and surface binding assays) in a single global analysis. The main purpose of the platform development was to reduce the discrepancies between the thermodynamic parameters obtained using different devices and setups (e.g. the use of different sample volume, concentrations, immobilization of the template, etc...). The SEDPHAT results presented in the present chapter concern only calorimetry data in order to perform a global analysis of several measurements, including repetitions of the performed direct and reverse titrations, increasing therefore the confidence in the binding parameters obtained individually with NanoAnalyze software.

4. ITC data and their evaluation

The following subsections illustrate the extraction of thermodynamic parameters and association constant from the experimental raw data for one-site and two-sites binding complexes in different non-aqueous solvents.

4.1 1:1 Complexes in different solvents and calorimetric heat capacity

Molecular recognition processes are the archetypal reactions in various domains going from life science to technology and the design of a suitable target which binds the other partner with specificity remains challenging nowadays. The study of the binding complexes presented herein was originally motivated by the need to optimize the design of molecularly imprinted polymers [55] by characterizing the affinity and the complete thermodynamic profile of the monomer-target interaction in the solvent used for the synthesis of the final polymer. A better comprehension of the interactions and energies

involved in the preorganization of the monomers around the target could improve their synthesis protocols by selecting monomers with high affinity for the target.

The feasibility of elucidating the thermodynamic parameters for a 1:1 binding model using stepwise titration experiments is first demonstrated with the interaction between benzoic acid (**1**), a food antimicrobial, and *N*-[3-(dimethylamino)propyl]methacrylamide (**2**), a monomer, in methanol (Figure 2). In water at 25°C, **1** shows a pKa of ~4.2 (49)

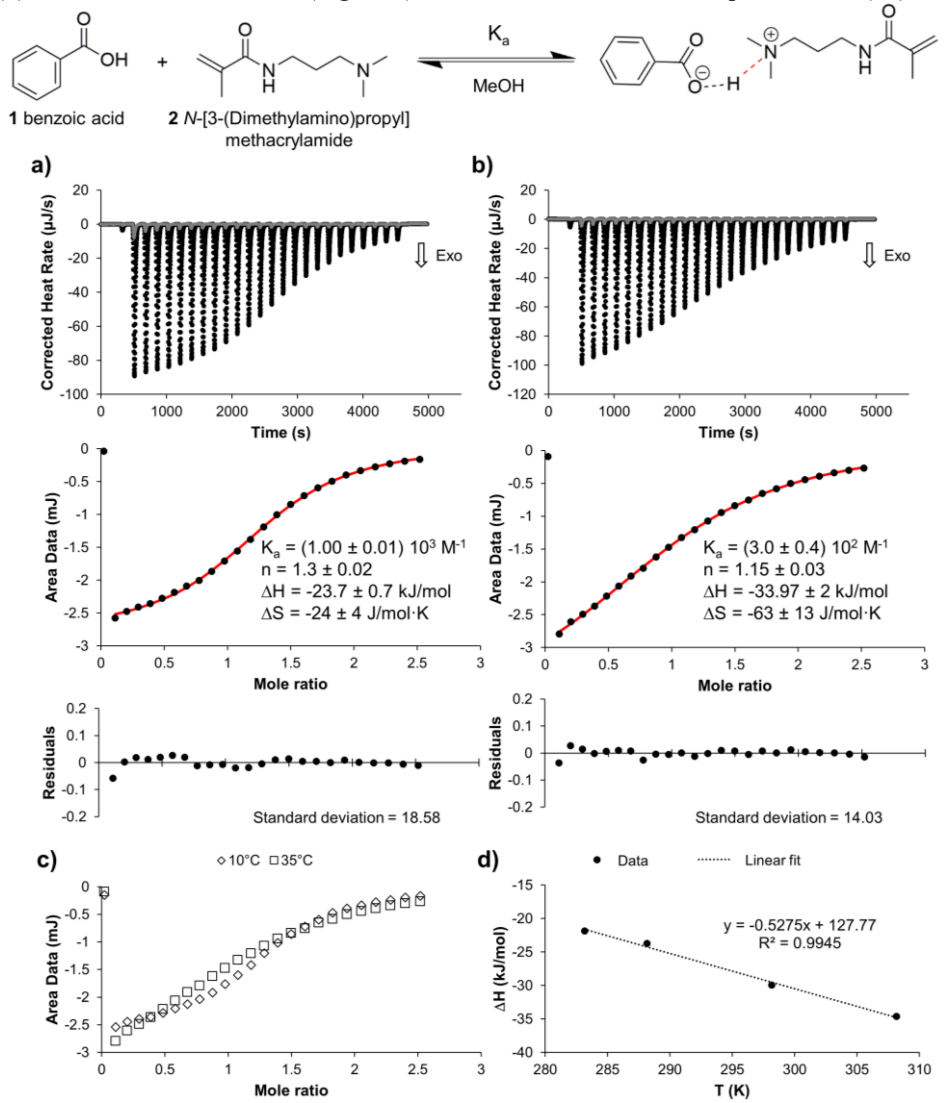

Figure 2: ITC titration of **2** into **1** in MeOH at 15 (a) and 35°C (b) as filled black circles. The dilution of **2** into MeOH is also shown as grey filled circles. The middle thermogram shows the integrated heat data as filled black circles and their nonlinear fitting using the 1:1 binding model as red continuous line. c) Integrated corrected data at 10 and 35°C. d) Linear fit of the calorimetric ΔH values versus temperature which gives access to the change in heat capacity, ΔC_p ~ -0.5 kJ/mol·K.

whereas **2** is a typical amine base characterized by a pKa of ~9.2. In methanol and other organic solvents, the pKa cannot be defined but it is expected that **1** and **2** behave as a strong Lewis acid and base, respectively. Qualitative evidence of the interaction between benzoic acid and 2-dimethylaminoethyl methacrylate-based copolymers has been provided by infrared (IR) and ^{1}H NMR spectroscopies (50). ^{1}H NMR spectra recorded for different

molar compositions of benzoic acid:copolymer containing amine groups in acetone showed that carboxyl-amine interaction causes a shift of the aromatic proton resonances to high field (small ppm values) whereas protons near the amine group shift to low field (big ppm values). These chemical shifts suggest that the carboxyl-amine complexation is associated with an increase in electron density for the carboxyl and a decrease of the electron density for the amine group, results consistent with the formation of a contact ion pair stabilized by attractive electrostatic forces and H-bonding. The same conclusions are reached by analyzing the IR spectra of the mixtures in acetone. For these complexes in chloroform and acetone solvents, it was stated that the excess of benzoic acid tends to self-association producing therefore benzoic acid dimers in addition to the benzoic acid-amine complex.

Figures 2 and 3 display the calorimetry data for the interaction between benzoic acid (**1**) and *N*-[3-(dimethylamino)propyl]methacrylamide (**2**) in methanol and acetonitrile, respectively. In order to estimate the heat capacity changes, the heat reaction response has been measured in methanol over a temperature range between 10 and 35°C. The top panels in Figure 2a and b indicate that the complexation is exothermic over the full temperature range spanned. The middle and the bottom panels show the integrated experimental heat data fitted with the 1:1 independent binding model and the residuals which describe the differences between the interaction model and the measured data. In all experiments, 60 mM **2** were titrated into 8 mM **1** except otherwise indicated. Table 2 summarizes the ensemble of thermodynamic parameters together with the stoichiometry and the association constant derived using a 1:1 independent binding model at each temperature. The calculated *c*-value is also shown and falls in the range 2-20. The concentration conditions have been optimized using the tool "ITC Experiment Design" from NanoAnalyze at 25°C for a *c*-value ~ 10. A greater *c*-value would have required higher concentrations for benzoic acid and therefore would have prevented us from carrying out the reverse titration owing to benzoic acid reduced solubility in MeOH above 60 mM. In parallel, to check the accuracy of the **1**-**2** affinity and thermodynamics parameters obtained by ITC, a global fit analysis for both direct (60 mM **2** into 8 mM **1**) and reverse (60 mM **1** into 8 mM **2**) titrations in MeOH at 25°C has also been performed with the open source SEDPHAT platform. First, the ITC data have been integrated using the NITPIC software which also allows to subtract the corresponding dilution for each direct and reverse titration dataset and gives access to the stoichiometry parameter. Second, the direct and indirect NITPIC datasets were integrated and saved in a SEDPHAT configuration file. The data were then fitted with the one-site binding model and the statistics of the thermodynamic parameters calculated for a confidence level at 95%. The results obtained with SEDPHAT (Table 2) are almost identical to the ones obtained for the direct titration with NanoAnalyze. SEDPHAT contains explicit factors which can account for errors in the active concentrations. Their inspection for the individual analysis of both and direct titration data suggests an error in concentrations notably for the indirect titration. This might explain the bigger estimations of the stoichiometry and enthalpy change in the case of reverse titration.

The results summarized in Table 2 show that the **1**-**2** complexation is an exothermic ($\Delta H < 0$) and enthalpy-driven ($|\Delta H| > |T\Delta S|$) process at all temperatures and experimental conditions studied. K_a decreases with increasing temperature while ΔH becomes more exothermic as the temperature rises. The $|\Delta S|$ show also a tendency to increase with temperature. Within the experimental uncertainties, the calculated $|\Delta S|$ values, which range within 20 and 50 kJ/mol·K, are in good agreement with the expected entropy change characterizing the ion pair formation from neutral reactants in polar solvents [56,57]. The decrease of the association constant by about one order of magnitude between 10 and 35°C is particularly relevant for the design of molecularly imprinted polymers because their synthesis is usually performed at temperatures higher than the ones used here (50 to 70°C). It therefore suggests the importance of probing the interaction between the target and the functional monomer at the synthesis temperature.

Table 2: Best-fit thermodynamic parameters from ITC measurements for the **1**-**2** complex in methanol.

T °C	K_a M^{-1}	n	ΔH [a]	ΔS [a]	ΔG [a]	*c* [b]
10	(1.5 ± 0.1) 10^3	1.36 ± 0.02	-21.3 ± 0.4	-14 ± 4	-17.3 ± 0.7	16
	(1.3 ± 0.1) 10^3	1.30 ± 0.02	-22.4 ± 0.5	-19 ± 5	-17.0 ± 0.8	14
15	(1.00 ± 0.01) 10^3	1.30 ± 0.02	-23.7 ± 0.7	-24 ± 4	-16.7 ± 0.1	10
25	(6.7 ± 0.9) 10^2	1.07 ± 0.02	-30 ± 1	-46 ± 9	-16 ± 1	6
	(5.8 ± 0.3) 10^2 [c]	1.07 ± 0.01 [c]	-21.9 ± 0.4 [c]	-20 ± 4 [c]	-15.9 ± 0.5 [c]	6 [c]
	(7.0 ± 0.1) 10^2 [d]	1.16 ± 0.03 [d]	-25 ± 1 [d]	-28 ± 7 [d]	-17 ± 1 [d]	6 [d]
	(7.0 ± 0.1) 10^2 [d]	1.13 ± 0.04 [d]	-26 ± 2 [d]	-32 ± 9 [d]	-17 ± 1 [d]	6 [d]
	(6.4 ± 0.6) 10^2 [e]	1.1 ± 0.6 [e]	-30.0 ± 0.5 [e]	-46 ± 8 [e]	-16.1 ± 0.9 [e]	-
	(2.5 ± 0.4) 10^2 [f]	1.14 ± 0.03 [f]	-33 ± 2 [f]	-64 ± 15 [f]	-14 ± 2 [f]	2 [f]
35	(3.0 ± 0.4) 10^2	1.15 ± 0.03	-34 ± 2	-63 ± 13	-15 ± 2	3
	(2.7 ± 0.3) 10^2	1.15 ± 0.03	-35 ± 2	-67 ± 14	-14 ± 1	2

[a] kJ/mol, ΔS is given in J/mol·K; [b] calculated *c*-value; [c] 100 mM **2** into 10 mM **1**; [d] 60 mM **1** into 8 mM **2** (reverse titration); [e] global analysis done on direct and reverse datasets and performed with SEDPHAT platform [54], n value is calculated based on the values obtained in the individual analysis with NITPIC [58] as SEDPHAT employs a different parameter in its analysis; [f] in acetonitrile.

In order to estimate the heat capacity changes, the heat reaction response has been measured over a temperature range between 10 and 35°C. The analysis of the variation of ΔH as function of T (Figure 2d) allows to estimate a value for ΔC_p ~ -0.5 kJ/mol·K. Formally, for a simple equilibrium studied over a relatively narrow temperature range, ΔCp should be zero. Thus, these results suggest that the complexation process may be more complicated than initially assumed. Taken together, these results suggest that the **1**-**2** complex formation mechanism probably involves two or more coupled equilibria whose relative importance depends on temperature and reactant concentrations. For example, if at the concentrations used, a small fraction of the benzoic acid is in the dimeric form, the **1**-**2** acid/base complex formation requires the dissociation of the dimer and therefore a coupling of the two equilibria (complexation and dimerization). This can explain the discrepancies observed in n (which is clearly different of 1), ΔH and ΔS calculated at different temperatures (Figure 2a and b). Coupled equilibria may also explain the differences between "direct" and "reverse" titrations.

Figure 3 shows ITC titration of 60 mM of **2** in acetonitrile in 8 mM of **1** in the same solvent at 25°C. The thermodynamic parameters obtained from fitting the experimental data are listed in Table 2. This study was performed to investigate the role of H-bond interactions in the thermodynamics of the reaction. Acetonitrile and methanol show similar dielectric constants (36.6 and 33.0, respectively) and thus should exhibit similar abilities to stabilize the ionic product (relative to the reactants). However, both solvents differ markedly in their ability to form H-bonds. Methanol, a protic solvent, should further stabilize reactants and reaction product through the formation of such bonds. However, a comparative analysis of the ΔG values (ΔH and ΔS) obtained in acetonitrile and methanol at 25°C (see Table 2) shows that, within experimental uncertainties, they are practically identical. These results suggest that H-bonds do not preferentially stabilize neither the reactants nor the complex, and therefore, they are not determinant in the thermodynamics of the complexation process.

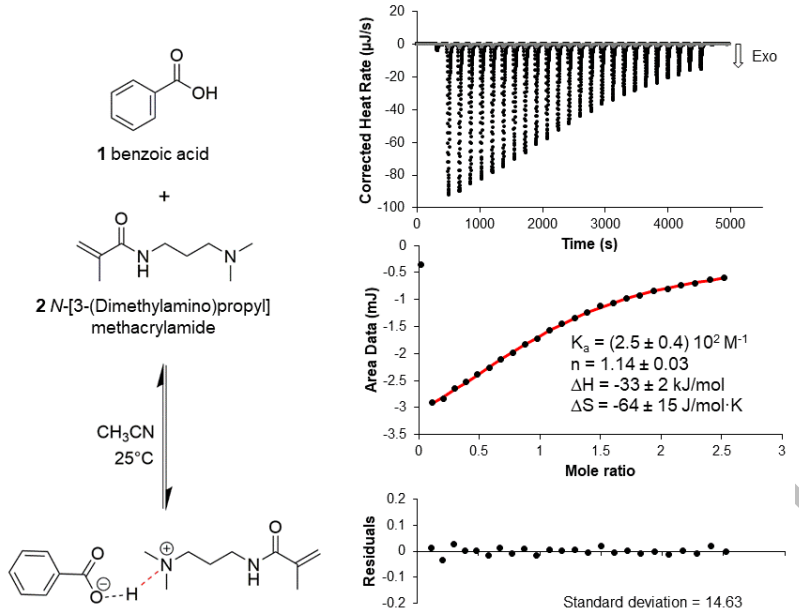

Figure 3: ITC titration of **2** into **1** in acetonitrile at 25°C as filled black circles. The dilution of **2** into acetonitrile is overlaid as grey filled circles. The middle thermogram shows the integrated heat data as filled black circles and the nonlinear fitting of the data using the 1:1 binding model as red continuous line.

The second complexation process explored by stepwise ITC titration concerns the interaction between the glucuronic acid (**4**), a sugar acid derived from glucose, and (4-acrylamidophenyl)amino methaniminium acetate (**5**), a polymerizable benzamidine salt, which can form with carboxylates stoichiometric non-covalent complexes characterized by affinities higher than 10^3 M^{-1} [59]. We previously studied the **4**-**5** complexation by ^{1}H NMR spectroscopy in DMSO-d_6 [60]. Job's plot [61,62] and titration experiments demonstrated the formation of a 1:1 complex with an affinity of 7.1 10^3 M^{-1}. The complex formation in MeOD/D_2O (4/1 v/v) gives slightly smaller chemical shift differences and an association constant of 4.4 10^3 M^{-1}.

Figure 4 displays the calorimetry data obtained at 25°C in MeOH/H_2O (4/1 v/v) for direct (i.e., monomer into the glucuronic acid) and reverse (i.e., glucuronic acid into the monomer) titrations. An inspection of the reaction scheme (top of Figure 4) suggests that the process can be considered as a displacement reaction (i.e., a reaction where glucuronic acid replaces acetate as a counter ion of the salt). The titration thermograms in top panels of Figure 4a and b show that the macroscopic experimental heat either changes from endothermic to exothermic (direct titration) or remains endothermic (reverse titration). The dilution of **4** and **5** is exothermic. The nonlinear fitting of the macroscopic heat data after dilution subtraction gives the thermodynamic parameters, the stoichiometry and the association constant reported in Table 3. The relatively small errors can be correlated with the calculated *c*-value, which is an order of magnitude higher than for the **1**-**2** complex described previously.

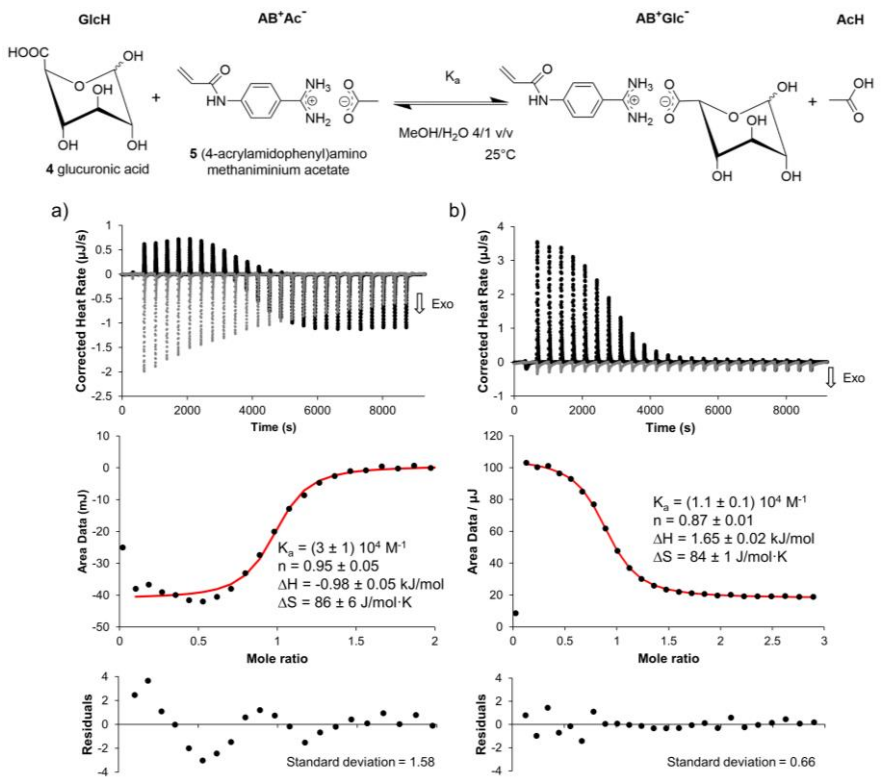

Figure 4: Direct (a) and reverse (b) titrations of AB^+Ac^- (**5**) into GlucH (**4**) in MeOH/H_2O (4/1 v/v) at 25°C as filled black circles. The dilutions of **4** and **5**, respectively, into MeOH/H_2O (4/1 v/v) are also shown as grey filled circles. The middle thermogram shows the integrated heat data as filled black circles and the nonlinear fitting of the data using the 1:1 independent binding model as red continuous line.

Table 3: Thermodynamic parameters of the **4**-**5** complex in MeOH/H_2O (4/1 v/v) at 25°C.

K_a M^{-1}	n	ΔH [a]	ΔS [a]	ΔG [a]	*c* [b]
(3 ± 1) 10^4 [c]	0.95 ± 0.05 [c]	-0.98 ± 0.05 [c]	86 ± 6 [c]	-26 ± 2 [c]	86 [c]
(1.1 ± 0.1) 10^4 [d]	0.87 ± 0.01 [d]	1.65 ± 0.02 [d]	84 ± 1 [d]	-23.3 ± 0.4 [d]	29 [d]

[a] kJ/mol, ΔS is given in J/mol·K; [b] calculated *c*-value; [c] 21 mM **5** into 3 mM **4** (direct titration); [d] 25 mM **4** into 3 mM **5** (reverse titration).

For both (direct and reverse) titrations, the enthalpy change (ΔH) is close to zero whereas the Gibbs free energy change (ΔG) is negative, which indicates a spontaneous process. Since T|ΔS| >> |ΔH|, the reaction is entropy driven. As we show below, the negative driving force of the displacement reaction is mainly due to the observed differences in the association constant (K') of the two acids. In water, the reported pKa are 4.75 [63] and 2.88 [64] for acetic and glucuronic acids, respectively. This difference in acidity is explained by the presence of one oxygen atom in the carbon α to the glucuronic -COOH group, which significantly weakens the O-H bond. The thermodynamics of the displacement reaction can be analyzed as a reaction occurring in consecutive stages. This is possible because Gibbs free energy is a state function of the system (i.e., it is independent pathway taken but only on the initial and final states) and therefore, the global displacement reaction (top of Figure 5) can be written as the sum of 3 hypothetical steps reaction characterized by their Gibbs free energies: ΔG_1, ΔG_2 and ΔG_3, so that $\Delta G = \Delta G_1 + \Delta G_2 + \Delta G_3$.

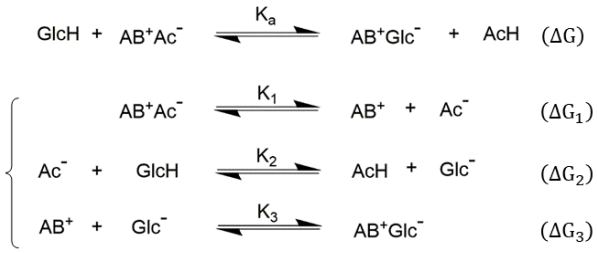

Figure 5: Global displacement reaction described as a 3 steps chemical process.

The first step describes to the dissociation of the AB^+Ac^- into the corresponding solvated free ions characterized by $\Delta G_1 > 0$. The second step is an acid-base reaction in which the acetate and the glucuronic acid exchange a proton for which the ΔG can be calculated as explained latter. Finally, the third step corresponds to the association of the glucoronate ion with the monomer counter ion to complete the displacement process and has a $\Delta G_3 < 0$. Although ΔG_1 and ΔG_3 are not identical, as they characterize the dissociation/association of different ion pairs, they will have similar orders of magnitude and we can assume that: $\Delta G_1 + \Delta G_3 \sim 0$. Based on this hypothesis, the main contribution to the global reaction should come from ΔG_2. The equilibrium constant for this process (K_2) can been determined from the pKa values to be ~ 80. Using the relationships of Eq 1, we obtain $\Delta G_2 \sim$ - 10 kJ/mol. Although this value is half of that obtained experimentally, it should be remembered that the K_2 was roughly calculated from the pKa obtained in water. The decreased dielectric constant in the MeOH/H_2O (4/1 v/v) mixture used in this study should enhance the differences in acidity between the two acids, making the process even more spontaneous.

3.2 Two-sites complexes

The involvement of more than one molecular process into a reaction is not always directly visible on the measured heat profile. The casual case where the two interaction mechanisms have an enthalpy that nicely emphasizes each inflexion of 1:2 (or 1:3) complexation is relatively rare. Figure 6 shows the example of a two-sites assembly with the interaction between the dimethylamino-based monomer and isophthalic acid, a target with two carboxylic groups, by putting it in mirror of the complex formed between the same monomer with benzoic acid. Both titrations have been carried out at 25°C in methanol.

The experimental heat response for a 2:1 complexation could be in theory approached with three different binding models (one-site independent, two-sites independent and two-sites sequential). Nevertheless, different arguments may help to restrict the plausible models: close inspection of the data to see if the two individual binding processes are clearly visible on the heat response, choice of the model with the smallest number of adjustable parameters, analysis of the nature of the functional groups of the interacting partners, interaction knowledge from other techniques, etc.

For all the thermograms in Figure 6, the binding isotherms were obtained as previously described by integrating the individual heat variation which results from the injection of the titrant. In both cases, initially a nonlinear least-squares regression analysis considering a single binding site was employed for both titrations. As represented in Figure 6a, the model fits well the data for the complex with benzoic acid, allowing to estimate the dissociation constant and the binding enthalpy while the stoichiometry value close to 1 confirmed the one-site interaction. In the case of the complex with the isophthalic acid, the one-site binding model is the simplest one to test with only 3 variable parameters and could represent a first acceptable choice if we assume the two carboxyl groups as chemically

equivalent. However, this assumption is not strictly true, since it has been reported that the pKa values of the two carboxyl groups of **3** at 25°C in water are: pK_{a1} = 3.46, pK_{a2} = 4.46 (ref). Therefore, this model is expected to estimate a stoichiometry of 2 together with a binding enthalpy (ΔH) and an association constant (K_a) as an average of the two complexation events. Table 4 collects the thermodynamic parameters obtained by nonlinear fitting the data with the one-site binding model. It is important to note that the thermodynamic parameters shown in Table 4 are per mole of binding sites (n = 2), so the global association constant (which considers full site occupancy) is $(K_a)^2 \sim 10^5\ M^{-2}$ and the global values of ΔG, ΔH and ΔS are twice those reported, i.e.: ~ -(28 ± 4) and -(34 ± 2) kJ/mol and ~ -(20 ± 20) kJ/mol·K, respectively.

The sequential two-sites model was also employed to approach the experimental ITC data. The evolution of the residuals and the decrease of the standard deviation suggest that the sequential two-sites binding model better approximates the experimental titration data. This model assumes the existence of two distinct binding sites in **3** with 1:1 stoichiometry each (i.e., the population of type 1 sites and type 2 sites in the sample is identical). The fitting of the experimental data to the model therefore provides 4 thermodynamic parameters, 2 for the initial stage (occupancy of site 1) and 3 for the second stage (occupancy of site 2). Results are summarized in Table 4. Again, the global equilibrium constant is the product of the K_a obtained at each step ($K_{a1}xK_{a2}$) ~ $10^5\ M^{-2}$, which is in full agreement with the result obtained using de 1:1 model. Similarly, the overall ΔG, ΔH and ΔS are the sum of the individual contribution to give: ~ -(38 ± 6) and -(42 ± 4) kJ/mol and ~ -(50 ± 20) kJ/mol·K, respectively. Within the experimental uncertainties, these values are similar to the ones obtained using the simplest one-site independent model. When the results determined with the sequential model for the **3-2** reaction are compared with those obtained for the **1-2** reaction, modeled with the one-site independent model, some interesting aspects emerge. For example, the first reaction step between **2** and **3** is spontaneous and its ΔG ~ -17 kJ/mol is very similar to that obtained for the reaction of **2** with **1**, ΔG ~ -16 kJ/mol. However, such coincidence occurs due to the compensation between ΔH and ΔS values (see Table 4), the entropic change for the first step of the reaction being for the reaction **3-2** positive. The results also suggest that the second reaction step is slightly less spontaneous, but is accompanied by a very large negative enthalpy and entropy change. Additional experimental data are required to better understand this system.

We should also mention that the two-sites independent model has also been tested but it has been discarded in the end as it contains the highest number of adjustable parameters (6 in total) and was giving unrealistic stoichiometries for the two sites.

Table 4: Thermodynamic parameters obtained by nonlinear fitting of heat data corresponding to the titration of 60 mM **2** into 8 mM **1** (first row) and 150 mM **2** into 10 mM **3** (last two rows) in MeOH at 25°C.

	K_a M^{-1}	**n**	**ΔH [a]**	**ΔS [a]**	**ΔG [a]**	***c* [b]**
1:1	(6.5 ± 0.9) 10^2	1.07 ± 0.02	-30 ± 1	-46 ± 4	-16 ± 1	6
2:1 [c]	(3.2 ± 0.6) 10^2	2.05 ± 0.02	-17.4 ± 0.9	10 ± 10	-14 ± 2	7
2:1 [d]	(1.0 ± 0.3) 10^3 (1.0 ± 0.2) 10^2	1 1	-16.6 ± 0.6 -26 ± 4	3 ± 8 -50 ± 20	-17 ± 2 -11 ± 4	-

[a] kJ/mol except for ΔS which is given in J/mol·K; [b] calculated *c*-value; [d] one-site independent binding model; [e] sequential two-sites binding model.

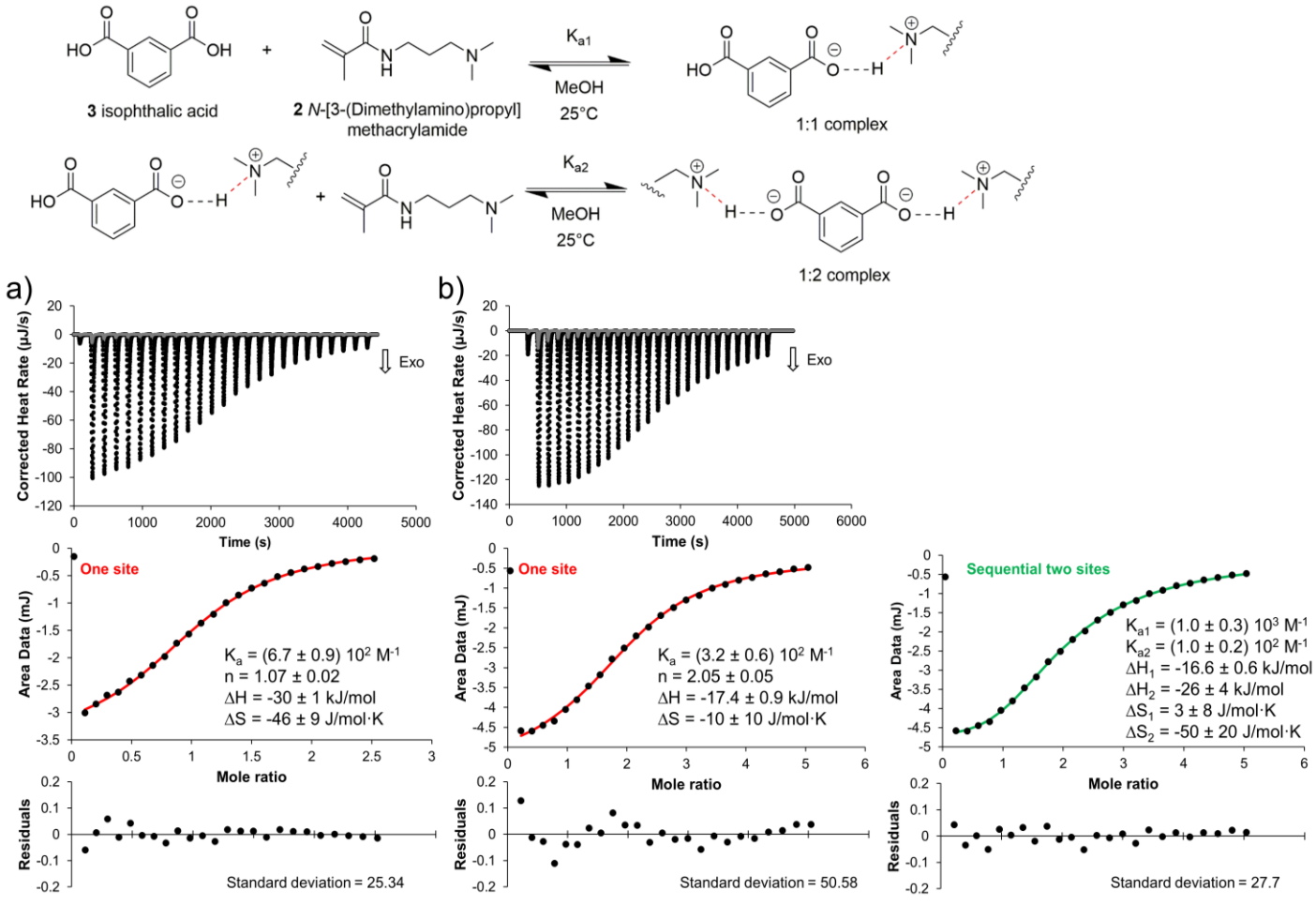

Figure 6: ITC titration for 1:1 and 1:2 complexes in methanol at 25°C. a) 2 into 1 and b) 2 into (3) titrations as black filled circles. The dilution of 2 into methanol is shown as grey filled circles on the top graphs as well. The middle thermogram shows the integrated heat data as filled black circles and the nonlinear fitting of the data using the one-site binding model as red continuous line or the sequential two-sites binding model for the interaction with isophthalic acid (right side) as green continuous line.

Conclusion and perspectives

Isothermal calorimetry is a label free non-destructive technique that became over the years the method of choice for most binding studies in solution. Compared to other dedicated spectroscopic techniques like nuclear magnetic resonance, infrared spectrometry or fluorimetry, which require a series of experiments to extract site-specific stoichiometry and affinity information, ITC gives access - in a single experiment – to a complete thermodynamic picture of the overall interaction mechanism. The continuous development of the technique led to highly sensitive instruments capable to detect small amounts of samples. For example, isothermal micro- and nano-calorimetry can measure tiny heat changes and became an important method for the thermodynamics profile analysis of chemical and biochemical reactions, solvation and dissolution processes. The automation of the entire experimental process with the new generation of calorimeters optimizes not only the use of the calorimeter but also increases the number of samples that can be studied. In parallel, considerable efforts have been made to propose various binding models and softwares with powerful routines for the optimization of experimental conditions (notably in terms of concentrations).

Despite the widespread application of ITC to probe interactions between biomolecules, the technique is hardly ever used for the characterization of the complexation of small molecules, especially when the titration is performed in organic solvents. Herein, we presented few examples that support the high potential of ITC for the study of interactions between small molecules in methanol, acetonitrile and methanol/water mixture on a Nano ITC Low Volume device (TA Instruments), with an emphasis on both simple (1:1) and more complex (1:1 and 1:2) interaction mechanisms.

In addition to the binding studies at equilibrium, ITC provided promising results for the investigation of reaction kinetics, irreversible reactions, reactions under pressure, etc. The field of application of isothermal calorimetry is continuously expanding from pharmacology to life science, clinical medicine, environmental science, biotechnology, ecology, etc.

Acknowledgments

The authors thank Jacques Loubens at TA Instruments, Waters, France for his kind assistance with the ITCRun and data analysis NanoAnalyze softwares. We are grateful to Bernadette Tse Sum Bui for kindly providing the monomer (4-acrylamidophenyl)-aminomethaminium acetate. We thank the European Regional Development Fund and the Region of Picardy (CPER 2007-2020). L.D. acknowledges financial support from the European Commission (project NOSY for New Operational Sensing sYstems, Grant agreement ID 653839, H2020-EU.3.7), the Hauts-de-France Region, the European Regional Development Fund (ERDF) 2014/2020 and Idex Sorbonne Université Investissements d'Avenir (2019/2020 EMERGENCE program).

Conflict of Interest

The authors declare no conflict of interest.

References

1. Christensen JJ, Izatt RM, Hansen LD. New precision thermometric titration

calorimeter. Rev Sci Instrum. 1965;36(6):779–83. https://doi.org/10.1063/1.1719702
2. Hansen LD, Christensen JJ, Izatt RM. Entropy titration. A calorimetric method for the determination of ΔG, ΔH and ΔS. Chem Commun. 1965;70(3):36–8. https://doi.org/10.1039/C19650000036
3. Chaires JB. Calorimetry and thermodynamics in drug design. Annu Rev Biophys. 2008;37:135–51. https://doi.org/10.1146/annurev.biophys.36.040306.132812
4. Rizzuti B, Lan W, Santofimia-Castaño P, Zhou Z, Velázquez-Campoy A, Abián O, et al. Design of inhibitors of the intrinsically disordered protein nupr1: Balance between drug affinity and target function. Biomolecules. 2021;11(10):1–19. https://doi.org/10.3390/biom11101453
5. Hughes JP, Rees S, Kalindjian SB, Philpott KL. Principles of early drug discovery. Br J Pharmacol. 2011;162(6):1239–49. https://doi.org/10.1111/j.1476-5381.2010.01127.x
6. Linkuvienė V, Krainer G, Chen W-Y, Matulis D. Isothermal titration calorimetry for drug design: Precision of the enthalpy and binding constant measurements and comparison of the instruments. Anal Biochem. 2016;515:61–4. https://doi.org/10.1016/j.ab.2016.10.005
7. Ladbury JE, Klebe G, Freire E. Adding calorimetric data to decision making in lead discovery: a hot tip. Nat Rev Drug Discov. 2010;9(1):23–7. https://doi.org/10.1038/nrd3054
8. Velazquez-Campoy A, Luque I, Freire E. The use of isothermal titration calorimetry in drug design: Applications to high affinity binding and protonation/deprotonation coupling. Netsu Sokutei. 2001;28(2):68–73. https://doi.org/10.11311/jscta1974.28.68
9. Freire E. Do enthalpy and entropy distinguish first in class from best in class? Drug Discov Today. 2008;13(19):869–74. https://doi.org/10.1016/j.drudis.2008.07.005
10. Falconer RJ, Schuur B, Mittermaier AK. Applications of isothermal titration calorimetry in pure and applied research from 2016 to 2020. J Mol Recognit. 2021;34(10). https://doi.org/10.1002/jmr.2901
11. Vander Meulen KA, Horowitz S, Trievel RC, Butcher SE. Measuring the kinetics of molecular association by isothermal titration calorimetry. Methods Enzymol. 2016;567:181–213. https://doi.org/10.1016/bs.mie.2015.08.012
12. F.P. Schmidtchen, Isothermal titration calorimetry in supramolecular chemistry, in: Anal. Methods Supramol. Chem., John Wiley & Sons, Ltd, 2006: pp. 55–78. https://doi.org/10.1002/9783527610273.ch3
13. Biedermann F, Schneider H, Platz H. Experimental binding energies in supramolecular complexes. Chem Rev. 2016;116:5216–300. https://doi.org/10.1021/acs.chemrev.5b00583
14. Wang Y, Wang G, Moitessier N, Mittermaier AK. Enzyme Kinetics by Isothermal titration calorimetry: Allostery, inhibition, and dynamics. Front Mol Biosci. 2020;7:1–19. https://doi.org/10.3389/fmolb.2020.583826
15. Di Trani JM, Moitessier N, Mittermaier AK. Measuring rapid time-scale reaction kinetics using isothermal titration calorimetry. Anal Chem. 2017;89(13):7022–30.
16. Di Trani JM, De Cesco S, O'Leary R, Plescia J, Do Nascimento CJ, Moitessier N, et al. Rapid measurement of inhibitor binding kinetics by isothermal titration calorimetry. Nat Commun. 2018;9(1). http://dx.doi.org/10.1038/s41467-018-03263-3
17. Braissant O, Wirz D, Göpfert B, Daniels AU. Use of isothermal microcalorimetry to monitor microbial activities. FEMS Microbiol Lett. 2010;303(1):1–8. https://doi.org/10.1111/j.1574-6968.2009.01819.x
18. Medina S, Raviv M, Saadi I, Laor Y. Methodological aspects of microcalorimetry used to assess the dynamics of microbial activity during

composting. Bioresour Technol. 2009;100(20):4814–20. http://dx.doi.org/10.1016/j.biortech.2009.05.015
19. Gaisford S. Stability assessment of pharmaceuticals and biopharmaceuticals by isothermal calorimetry. Curr Pharm Biotechnol. 2005;6(3):181–91. https://doi.org/10.2174/1389201054022913
20. Kimura T, Matsushita T, Kamiyama T. Enthalpies of solution of aliphatic compounds in dimethyl sulfoxide. Thermochim Acta. 2004;416(1–2):129–34. https://doi.org/10.1016/j.tca.2003.02.001
21. Sugiura T, Ogawa H. Thermodynamic properties of solvation of aromatic compounds in cyclohexane, heptane, benzene, 1,4-dioxane, and chloroform at 298.15 K. J Chem Thermodyn. 2009;41(11):1297–302. http://dx.doi.org/10.1016/j.jct.2009.06.001
22. Korolev VP, Antonova OA, Smirnova NL, Kustov A V. Thermal properties of tetraalkylammonium bromides in several solvents. J Therm Anal Calorim. 2011;103(1):401–7. https://doi.org/10.1007/s10973-009-0639-6
23. Riveros DC, Martínez F, Vargas EF. Enthalpies of solution of methylcalix[4]resorcinarene in non-aqueous solvents as a function of concentration and temperature. Thermochim Acta. 2012;548:13–6. http://dx.doi.org/10.1016/j.tca.2012.08.022
24. Alves N, Bai G, Bastos M. Enthalpies of solution of paracetamol and sodium diclofenac in phosphate buffer and in DMSO at 298.15 K. Thermochim Acta. 2006;441(1):16–9. https://doi.org/10.1016/j.tca.2005.11.031
25. Badelin VG, Mezhevoi IN. The thermochemical characteristics of solution of L-cysteine and L-asparagine in aqueous 1,4-dioxane and acetone. Russ J Phys Chem A. 2009;83(7):1121–4. https://doi.org/10.1134/S0036024409070139
26. Mezhevoi IN, Badelin VG. Standard enthalpies of dissolution of L-alanine in the water solutions of glycerol, ethylene glycol, and 1,2-propylene glycol at 298.15 K. Russ J Phys Chem A. 2010;84(4):607–10. https://doi.org/10.1134/S0036024410040151
27. Badelin VG, Smirnov VI. The dependence of the enthalpy of solution of L-methionine on the composition of water-alcohol binary solvents at 298.15 K. Russ J Phys Chem A. 2010;84(7):1163–8. https://doi.org/10.1134/S0036024410070150
28. Smirnov VI, Badelin VG. Enthalpies of solution of glycylglycine and diglycylglycine in aqueous alcohols at 298.15 K. Thermochim Acta. 2008;471(1–2):97–9. https://doi.org/10.1016/j.tca.2008.01.020
29. Guseva GB, Antina E V, Berezin MB, V'yugin AI. Enthalpies of dissolution of cobalt(II) and copper(H) acetylacetonates in organic solvents. Russ J Phys Chem. 2005;79(6):908–11.
30. Vandyshev VN, Ledenkov SF. Thermochemical study of complexation and solvation in β-Alanine- Cu(NO3)2-Water-Ethanol system: 1. Enthalpy characteristics of complexing copper(II) ion with β-Alanine. Russ J Inorg Chem. 2011;56(3):479–83. https://doi.org/10.1134/S0036023611030259
31. Jóźwiak M, Madej-Kiełbik L. Effect of temperature on the process of complex formation crown ether 15C5 with Na+ in the (water + ethanol) mixture at temperatures from (293.15 to 308.15) K. Thermochim Acta. 2014;580:13–9. https://doi.org/10.1016/j.tca.2014.01.019
32. Usacheva TR, Pham Thi L, Terekhova I V., Kumeev RS, Sharnin VA. Application of isothermal titration calorimetry for evaluation of water-acetone and water-dimethylsulfoxide solvent influence on the molecular complex formation between 18-crown-6 and triglycine at 298.15 K. J Therm Anal Calorim. 2015;121(3):975–81. https://doi.org/10.1007/s10973-015-4630-0
33. Bernaczek K, Mielańczyk A, Grzywna ZJ, Neugebauer D. Interactions between fluorescein isothiocyanate and star-shaped polymer carriers studied by isothermal titration calorimetry (ITC). Thermochim Acta. 2016;641:8–13.

https://doi.org/10.1016/j.tca.2016.08.007
34. Arnaud A, Bouteiller L. Isothermal titration calorimetry of supramolecular polymers. Langmuir. 2004;20(16):6858–63. https://doi.org/10.1021/la049365d
35. Wadsö I, Goldberg RN. Standards in isothermal microcalorimetry: (IUPAC Technical Report). Pure Appl Chem. 2001;73(10):1625–39. https://doi.org/10.1351/pac200173101625
36. TA Instruments, Nano ITC. [Accessed 2022 Jan 15]. Available from: https://www.tainstruments.com/nano-itc/
37. Velázquez-Campoy A, Ohtaka H, Nezami A, Muzammil S, Freire E. Isothermal titration calorimetry. In: Current Protocols in Cell Biology. 2004. p. 1–24. https://doi.org/10.1002/0471143030.cb1708s23
38. Quin C. F. Advanced ITC techniques: The reverse titration. 2013. http://www.tainstruments.com/pdf/literature/MCAPN-2013-01_Advanced_ITC_Techniques-The_Reverse_Titration.pdf
39. Spuches AM, Kruszyna HG, Rich AM, Wilcox DE. Thermodynamics of the as(III)-thiol interaction: Arsenite and monomethylarsenite complexes with glutathione, dihydrolipoic acid, and other thiol ligands. Inorg Chem. 2005;44(8):2964–72. https://doi.org/10.1021/ic048694q
40. Wiseman T, Williston S, Brandts JF, Lin LN. Rapid measurement of binding constants and heats of binding using a new titration calorimeter. Anal Biochem. 1989;179(1):131–7. https://doi.org/10.1016/0003-2697(89)90213-3
41. Myszka DG, Abdiche YN, Arisaka F, Byron O, Eisenstein E, Hensley P, et al. The ABRF-MIRG'02 study: assembly state, thermodynamic, and kinetic analysis of an enzyme/inhibitor interaction. J Biomol Tech. 2003;14(4):247–69.
42. Bastos M, Velazquez-Campoy A. Isothermal titration calorimetry (ITC): a standard operating procedure (SOP). Eur Biophys J. 2021;50(3–4):363–71. https://doi.org/10.1007/s00249-021-01509-5
43. Campoy AV, Claro B, Abian O, Höring J, Bourlon L. A multi-laboratory benchmark study of isothermal titration calorimetry (ITC) using -Ca^{2+} and - Mg^{2+} binding to EDTA. Eur Biophys J. 2021;50:429–51. https://doi.org/10.1007/s00249-021-01523-7
44. Fisher HF, Singh N. Calorimetric determination of binding constants. Energ Biol Macromol. 1995;259:194–221. https://doi.org/10.1016/0076-6879(95)59045-5
45. Horn JR, Russell D, Lewis EA, Murphy KP. Van't Hoff and calorimetric enthalpies from isothermal titration calorimetry: Are there significant discrepancies? Biochemistry. 2001;40(6):1774–8. https://doi.org/10.1021/bi002408e
46. Mizoue LS, Tellinghuisen J. Calorimetric vs. van't Hoff binding enthalpies from isothermal titration calorimetry: Ba^{2+}-crown ether complexation. Biophys Chem. 2004;110(1–2):15–24. https://doi.org/10.1016/j.bpc.2003.12.011
47. Markova N, Hallén D. The development of a continuous isothermal titration calorimetric method for equilibrium studies. Anal Biochem. 2004;331(1):77–88. https://doi.org/10.1016/j.ab.2004.03.022
48. Degassing station. [Accessed 2022 Feb 4]. https://www.tainstruments.com/degassing-station/
49. Herrera I, Winnik MA. Differential Binding Models for Direct and Reverse Isothermal Titration Calorimetry. J Phys Chem A. 2016;120:2077–86. https://doi.org/10.1021/acs.jpcb.5b09202
50. Piñeiro Á, Muñoz E, Sabín J, Costas M, Bastos M, Velázquez-Campoy A, et al. AFFINImeter: A software to analyze molecular recognition processes from experimental data. Anal Biochem. 2019;577:117–34. https://doi.org/10.1016/j.ab.2019.02.031
51. Duvvuri H, Wheeler LC, Harms MJ. Pytc: Open-source python software for global analyses of isothermal titration calorimetry data. Biochemistry. 2018;57(18):2578–83. https://doi.org/10.1021/acs.biochem.7b01264

52. Gans P, Sabatini A, Vacca A. Simultaneous calculation of equilibrium constants and standard formation enthalpies from calorimetric data for systems with multiple equilibria in solution. J Solution Chem. 2008;37(4):467–76. https://doi.org/10.1007/s10953-008-9246-6
53. Le VH, Buscaglia R, Chaires JB, Lewis EA. Modeling complex equilibria in isothermal titration calorimetry experiments: Thermodynamic parameters estimation for a three-binding-site model. Anal Biochem. 2013;434(2):233–41. https://doi.org/10.1016/j.ab.2012.11.030
54. Zhao H, Piszczek G, Schuck P. SEDPHAT – A platform for global ITC analysis and global multi-method analysis of molecular interactions. Methods. 2015;76:137–48. http://dx.doi.org/10.1016/j.ymeth.2014.11.012
55. Nicholls IA. Thermodynamic considerations for the design of and ligand recognition by molecularly imprinted polymers. Chem Lett. 1995;24(11):1035–6. https://doi.org/10.1246/cl.1995.1035
56. Dogadkin DN, Soboleva I V., Kuz'min MG. Formation enthalpy and entropy of exciplexes with variable extent of charge transfer in solvents of different polarity. High Energy Chem. 2001;35(4):251–7. https://doi.org/10.1023/A:1017636612185
57. Solís C, Grosso V, Faggioli N, Cosa G, Romero M, Previtali C, et al. Estimation of the solvent reorganization energy and the absolute energy of solvation of charge-transfer states from their emission spectra. Photochem Photobiol Sci. 2010;9(5):675–86. https://doi.org/10.1039/b9pp00190e
58. Scheuermann TH, Brautigam CA. High-precision, automated integration of multiple isothermal titration calorimetric thermograms: New features of NITPIC. Methods. 2015;76:87–98. http://dx.doi.org/10.1016/j.ymeth.2014.11.024
59. Nestora S, Merlier F, Beyazit S, Prost E, Duma L, Baril B, et al. Plastic antibodies for cosmetics: molecularly imprinted polymers scavenge precursors of malodors. Angew Chem Int Ed. 2016;55:6252–6. https://doi.org/10.1002/anie.201602076
60. Panagiotopoulou M, Salinas Y, Beyazit S, Kunath S, Duma L, Prost E, et al. Molecularly imprinted polymer coated quantum dots for multiplexed cell targeting and imaging. Angew Chem Int Ed. 2016;55(29):8244–8. https://doi.org/10.1002/anie.201601122
61. Job P. Formation and stability of inorganic complexes in solution. Ann Chim. 1928;9:113–203.
62. Renny JS, Tomasevich LL, Tallmadge EH, Collum DB. Method of continuous variations: Applications of job plots to the study of molecular associations in organometallic chemistry. Angew Chem Int Ed. 2013;52(46):11998–2013. https://doi.org/10.1002/anie.201304157
63. Goldberg RN, Kishore N, Lennen RM. Thermodynamic quantities for the ionization reactions of buffers. J Phys Chem Ref Data. 2002;31(2):231–370. https://doi.org/10.1063/1.1416902
64. Wang HM, Loganathan D, Linhardt RJ. Determination of the pK(a) of glucuronic acid and the carboxy groups of heparin by 13C-nuclear-magnetic-resonance spectroscopy. Biochem J. 1991;278(3):689–95. https://doi.org/10.1042/bj2780689